Phase transformations in solids

Eutectoid
Massive
Spinodal decomposition
Ordering

MAURO PALUMBO

mauro.palumbo@unito.it
Dipartimento di Chimica
Università di Torino
Via Pietro Giuria 9 –10125 Torino

Eutectoid transformation

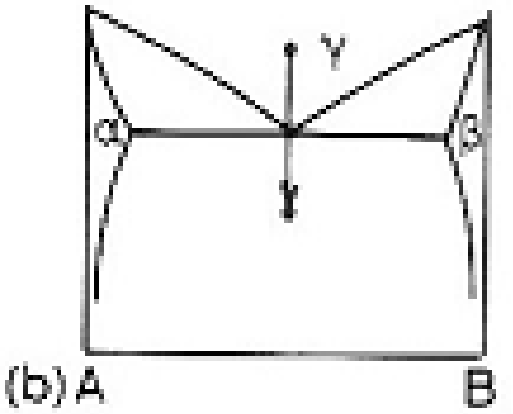

A eutectoid transformation is a type of phase transformation in which **a single solid phase transforms into two different solid phases upon cooling**. **It occurs via nucleation and growth. Growth is cooperative.**

$$\gamma \rightarrow \alpha + \beta$$

The **most studied case is austenite to pearlite**: $\gamma \Leftrightarrow \alpha + Fe_3C$. Pearlite nucleates on gb's, grows radially at constant rate. At low undercooling, small number of nuclei and fast growth. At large undercooling, faster nucleation but site saturation on gb's.

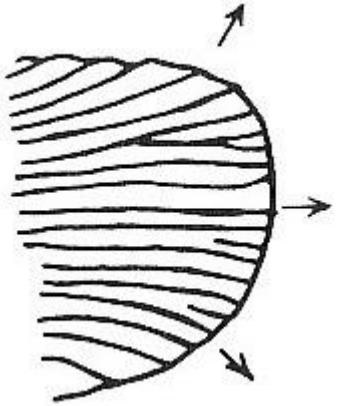

Eutectoid transformation

Either ferrite or cementite can nucleate first with an orientation relationship to one austenite grain γ_1.

K-S relationship for ferrite.

For orthorombic cementite:

$(100)_c//(1\underline{1}1)_\gamma$, $(010)_c//((110)_\gamma$, $(001)_c//(\underline{1}12)_\gamma$

Interface semicoherent with γ_1 and incoherent with γ_2.

Depletion/rejection of C atoms favours nucleation of the other phase. Process is re-iterated to form a colony.

Growth front proceeds via C diffusion in front of it.

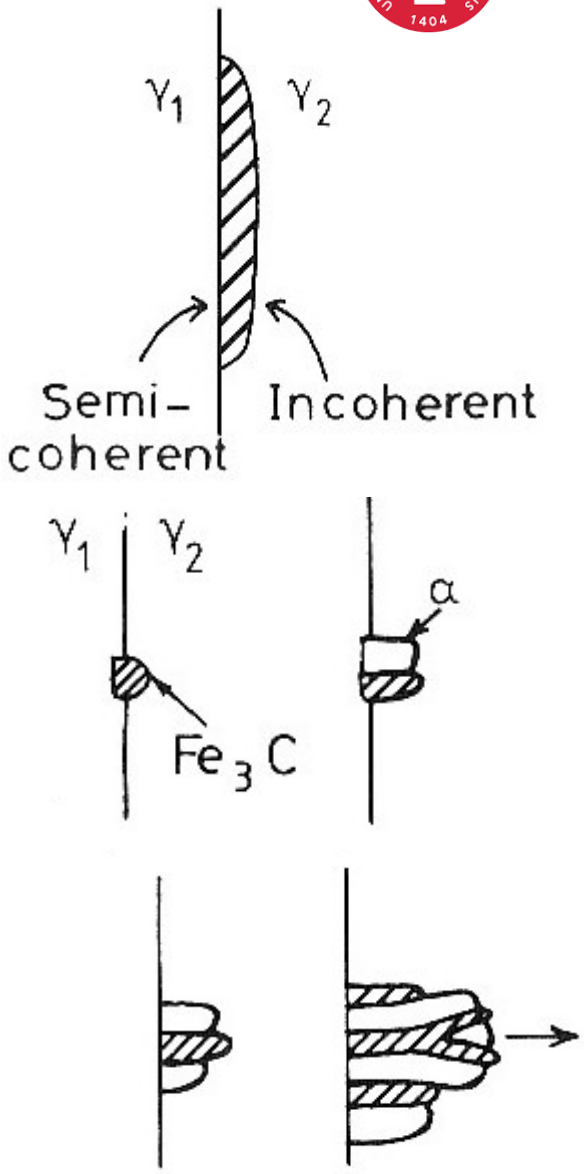

Eutectoid transformation

In hypo-(hyper-)eutectoid alloys, proeutectoid ferrite (cementite) already present on gb's: heterogeneous nucleation occurs on these.

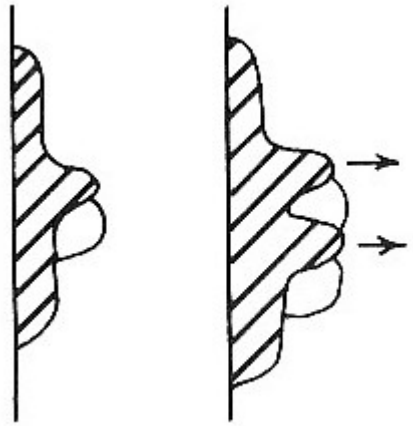

Rate of cooperative growth depends on concentration gradient ahead of phases and interlamellar spacing (i.e. diffusion distance), λ.

Both ΔX_C and λ depend on undercooling ΔT to a first approximation.

$$v = kD_C^{\gamma}\frac{\Delta X_C}{\lambda} \approx kD_C^{\gamma}(\Delta T)^2$$

Rate can be enhanced by C diffusion through interfaces.

Eutectoid transformation

Overall transformation described by TTT curve with maximum rate at about 550 °C. Other transformation features to be detailed later (bainite, M_S)

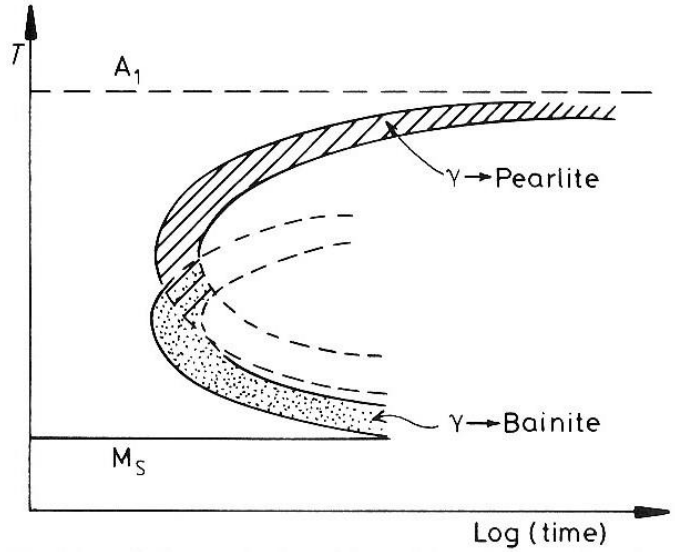

In off-eutectoid alloys (e. g., 0.6 %C) and high undercooling, supersaturated austenite can transform directly to pearlite.

Note that driving force for nucleation of both phases exists only below T_u.

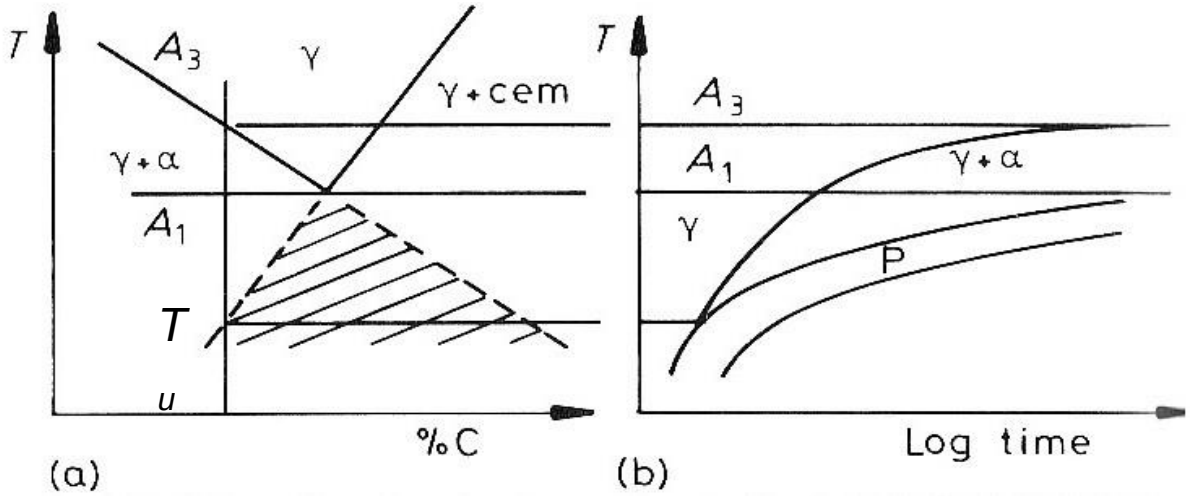

Bainitic transformation

Bainite contains ferrite and cementite. Microstructure is different from pearlite because of varied nucleation and growth mechanism: TTT curves for bainite and pearlite overlap in C-steels.

Upper (feathery) Bainite (~550 - 400 °C): ferrite nucleates with K-S orientation on γ_1; because of high nucleation rate groups of ferrite laths form. C is largely rejected into γ; finally cementite nucleates between bundles.

Contrary to pearlite, bainitic phases have orientation relationship with γ_2: semicoherent interface which has been described as glissile.

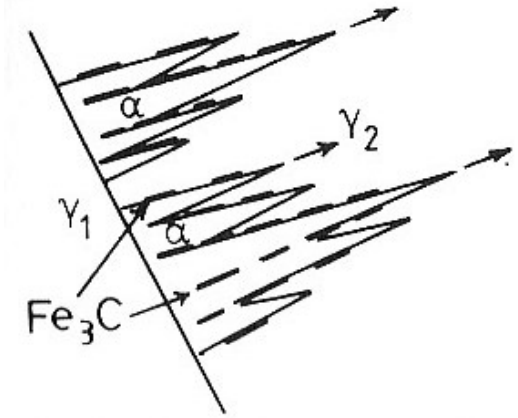

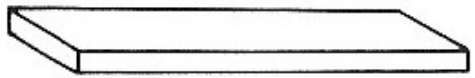

Bainitic transformation

Lower (acicular) bainite (~ 400 - 250 °C): ferrite plates nucleate and grow with supersaturation. Some carbide needles nucleate at γ-α interface, others precipitate from supersaturated ferrite.

The formation of both upper and lower bainite in a polished sample is shown to produce surface relief, possibly because of shear. Possible mixed characteristics of military and civilian transformations (this will be clearer later).

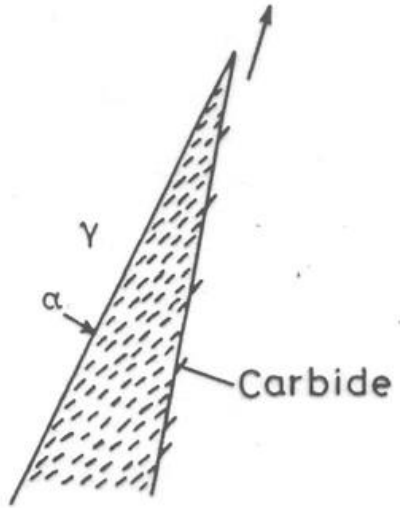

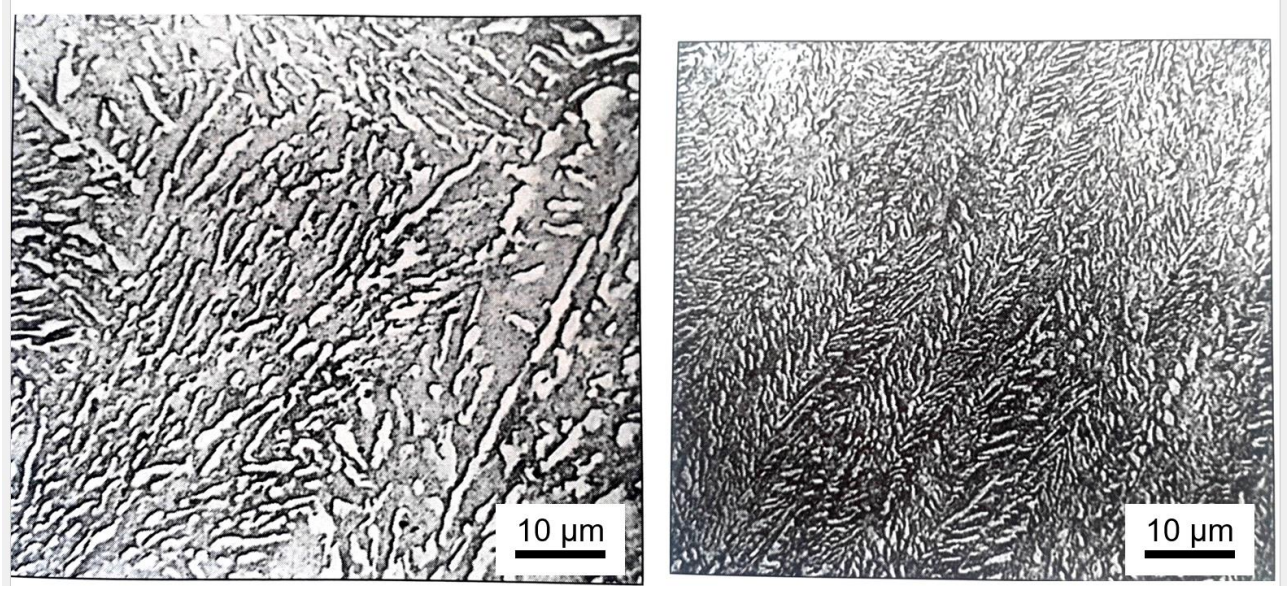

Upper (left) and lower (right) bainite microstructures at the microscope

Effect of alloying elements

(on phase transformations in the Fe-C system)

TTT curve is shifted to longer times for various reasons:

- Substitutional elements diffuse more slowly than interstitial C.
- Austenite stabilizers lowers eutectoid temperature (e.g. Mn, Ni, Cu) therefore at transformation temperature D is lower.
- Ferrite stabilizers (e. g. Cr, Mo, Si) increase eutectoid temperature but must partition between ferrite and cementite by substitutional diffusion even at high undercooling. Si diffuses along austenite/pearlite interface
- Carbide formers (e. g. Cr, Mo, Mn): also slow γ/α interface by solute drag and poison ferrite nucleation sites with carbides.

Effect of alloying elements

(on phase transformations in the Fe-C system)

TTT diagram for commercial steels (note: distinct “noses” for pearlite and bainite, shift in time with increase of amount of alloying elements)

a) 0.4 %C, 1 % Mn;

b) 0.4 %C, 1 % Mn, 0.9 % Cr

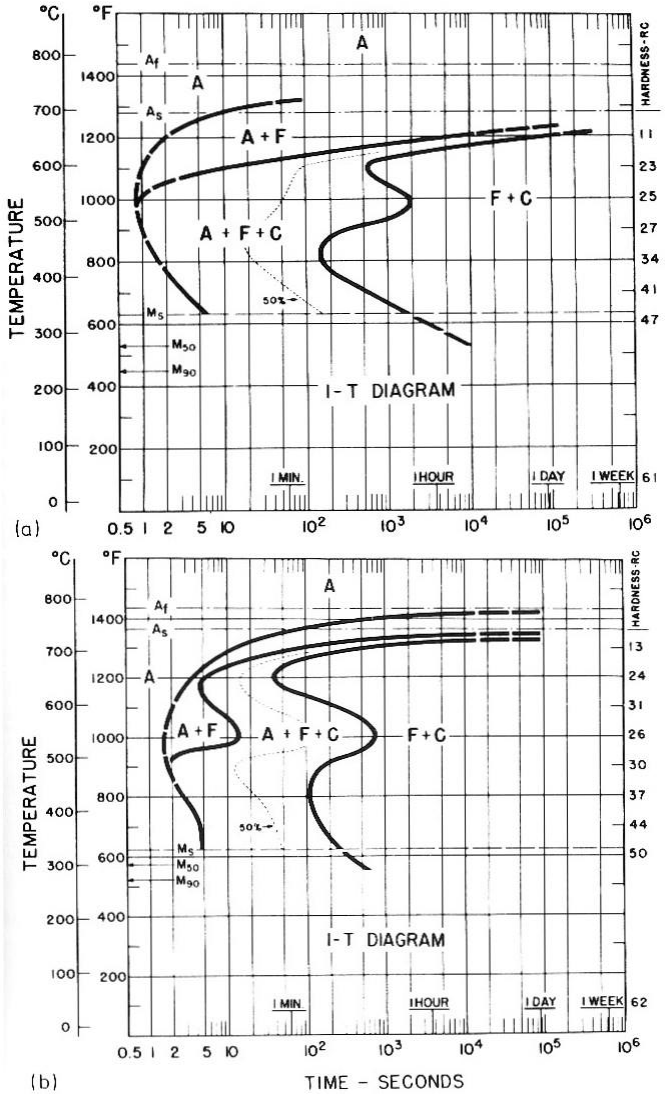

Effect of alloying elements

(on phase transformations in the Fe-C system)

further TTT diagram for commercial steels (note: shift in time and confinement of A-F curve in d))

c) 0.4 %C, 1 % Mn, 1 % Cr, 0.2 % Mo

d) 0.4 %C, 1 % Mn, 0.8 % Cr, 0.2 % Mo, 1.8 % Ni

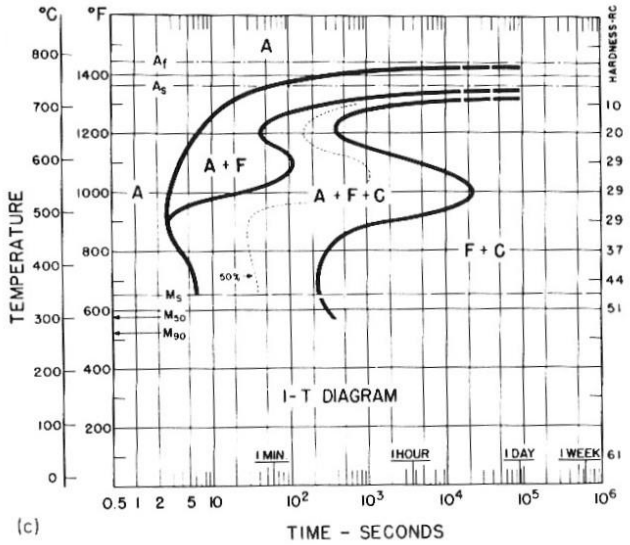

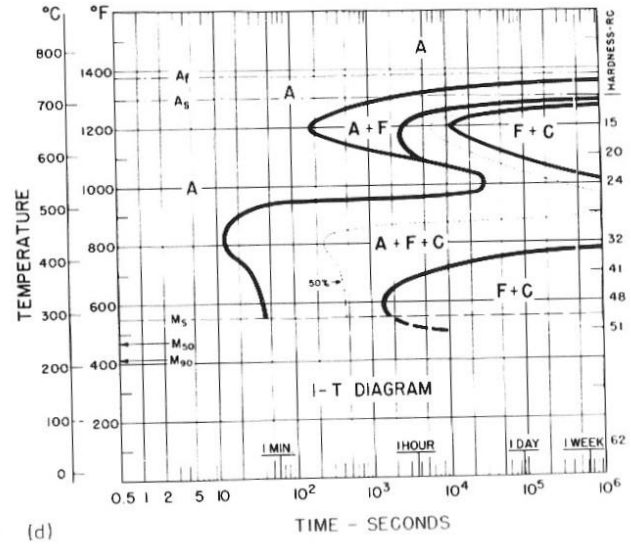

Continuous cooling curves (CCT)

Industrial heat treatments involve continuous cooling.

CCT curves shifted to lower temperature and times with respect to TTT.

CCT curves are shifted to lower temperature and times with respect to TTT.

Cooling curves in figure referred to a Jominy test.

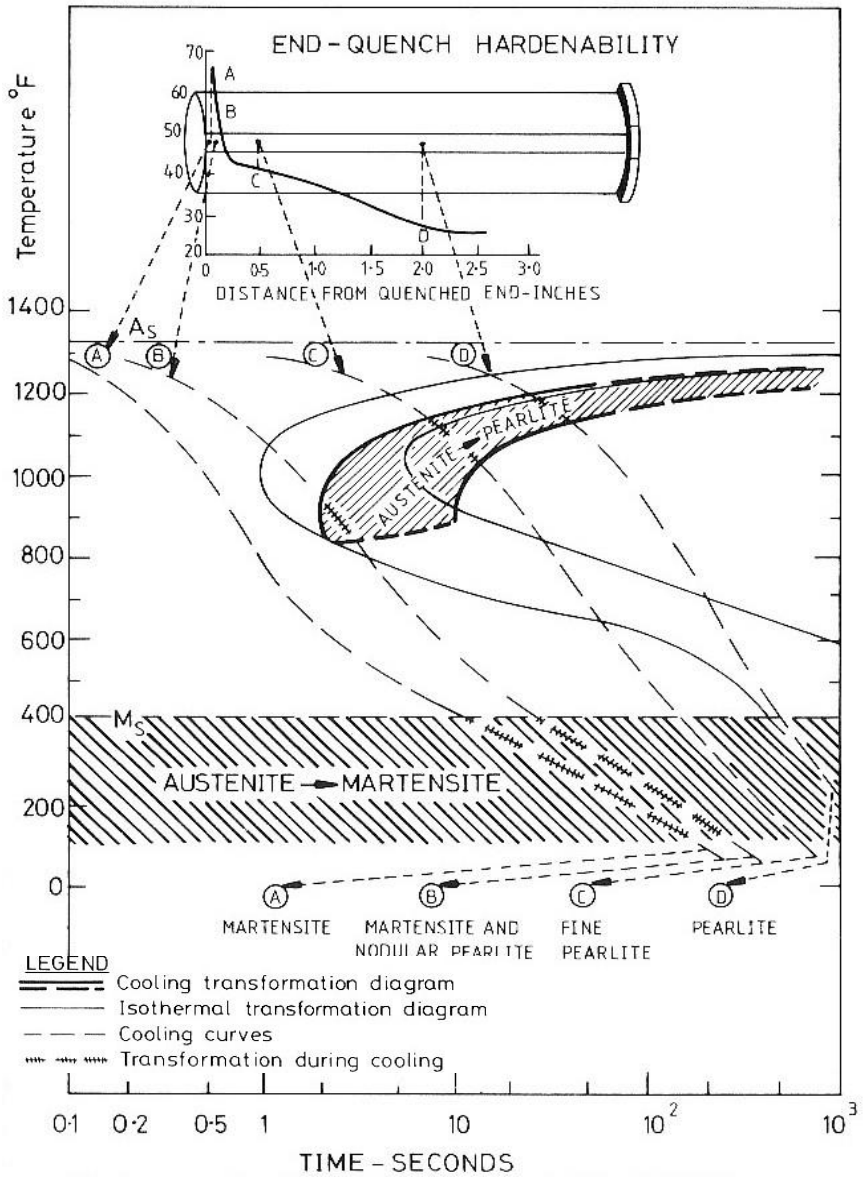

Continuous cooling curves (CCT)

CCT diagram for commercial steels

a) 0.39 %C, 0.72 % Mn, 0.23 % Si, 0.018 % S, 0.010 % P (note: increase in volume fraction of pearlite with increase in cooling rate)

b) 0.39 %C, 1.6 % Mn, 0.21 % Si, 0.024 % S, 0.010 % P (note shift in time and more effective quench)

Note recalescence in both cases.

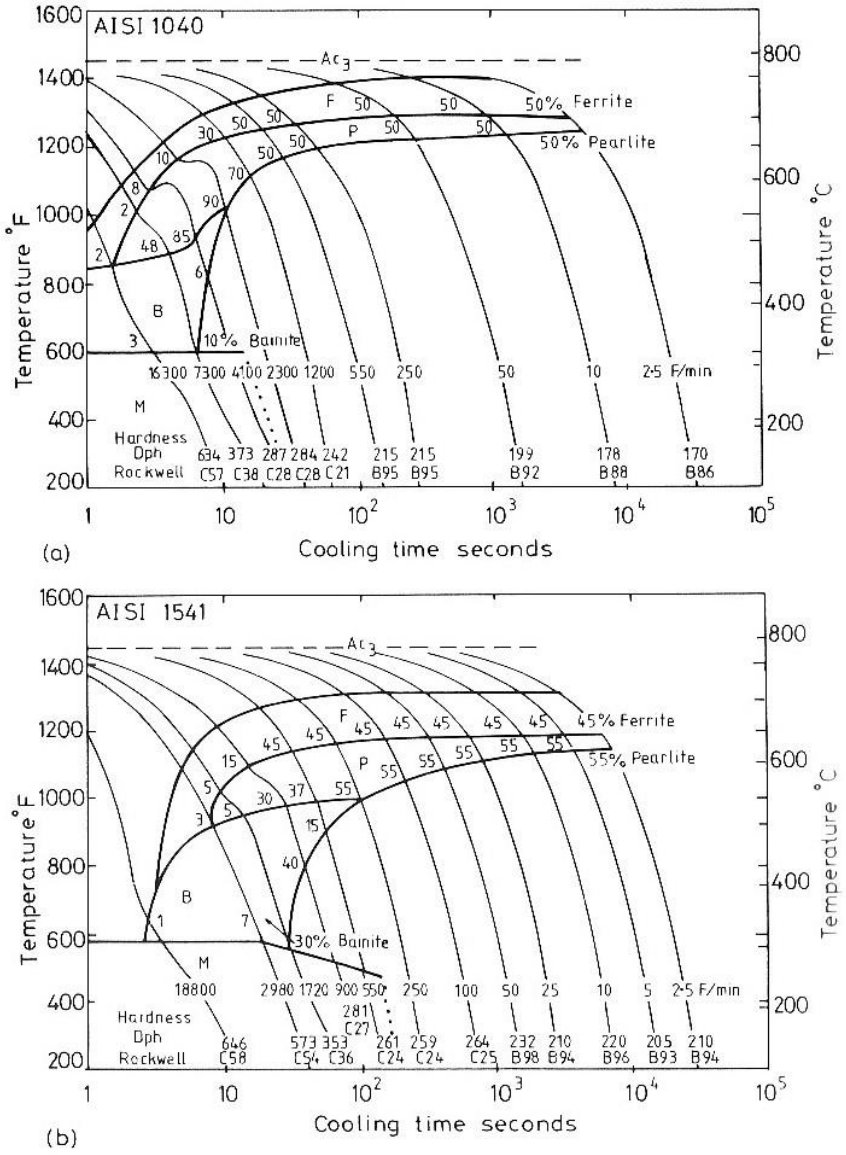

Quenching a solution: free energy

Extension of solid solubility at low temperature: basis for precipitation and spinodal decomposition in system with miscibility gap.

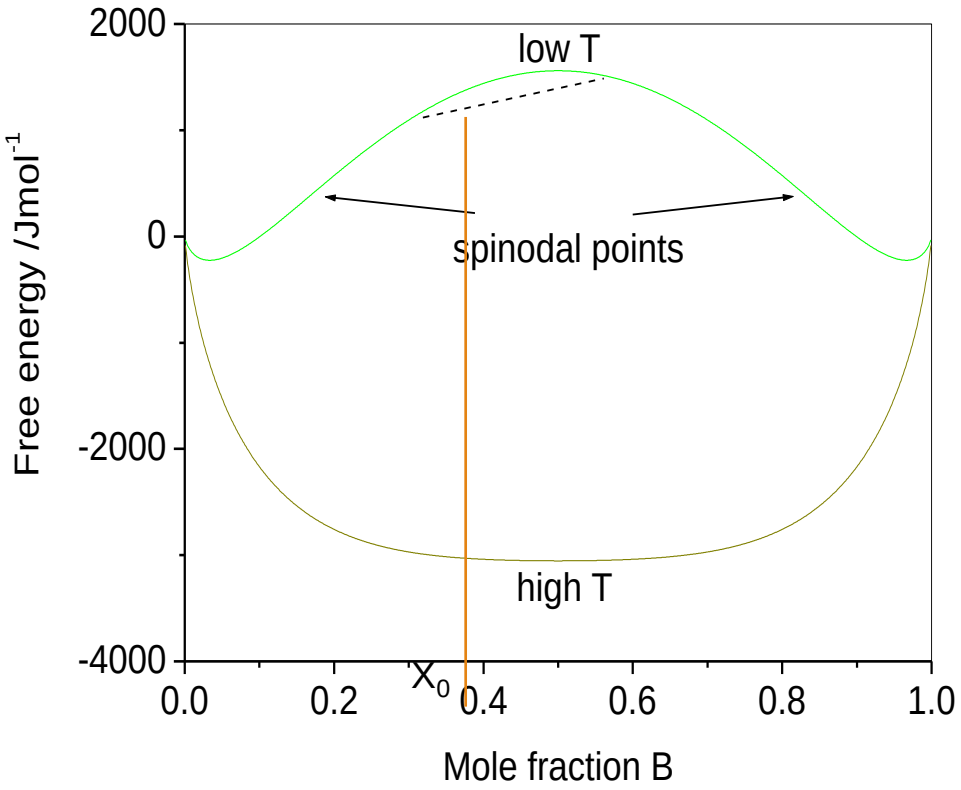

The high T solid solution, X_0, is quenched at low T: its free energy may fall within the spinodal points where

$d^2G < 0$ (instability condition).

Any fluctuation in composition produces decrease in free energy (dashed line)

Case for up-hill diffusion contrary to more frequent down-hill diffusion.

Spinodal decomposition

Second derivative of free energy vs composition: < 0 within the spinodal, > 0 outside it.

The phase diagram reports: equilibrium solvus and spinodal locus (dashed).
The free energy scheme shows the effect of local compositional fluctuations occurring in a metastable solid solution, e. g. X_0 (arrows): neighbouring zones have different free energy (black dots). The system free energyis given by their mechanical mixture (thin line).

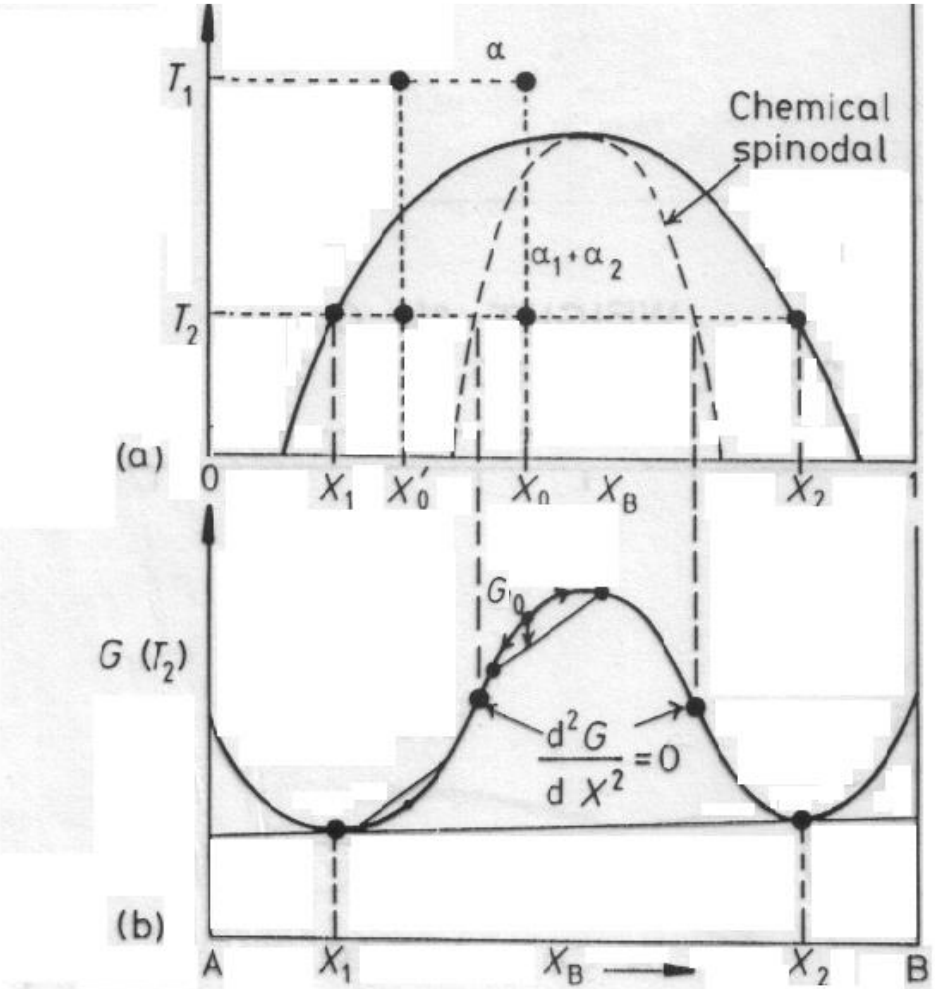

Fig. 5.38 Alloys between the spinodal points are unstable and can decompose into two coherent phases α_1 and α_2 without overcoming an activation energy barrier. Alloys between the coherent miscibility gaps and the spinodal are metastable and can decompose only after nucleation of the other phase.

Spinodal decomposition

Composition fluctuation for alloy, X_0‘, outside spinodal points within tangent points: free energy loss from G_0 (see position of thin line) de-stabilizes compositional gradient. Transformation occurs via nucleation and growth.

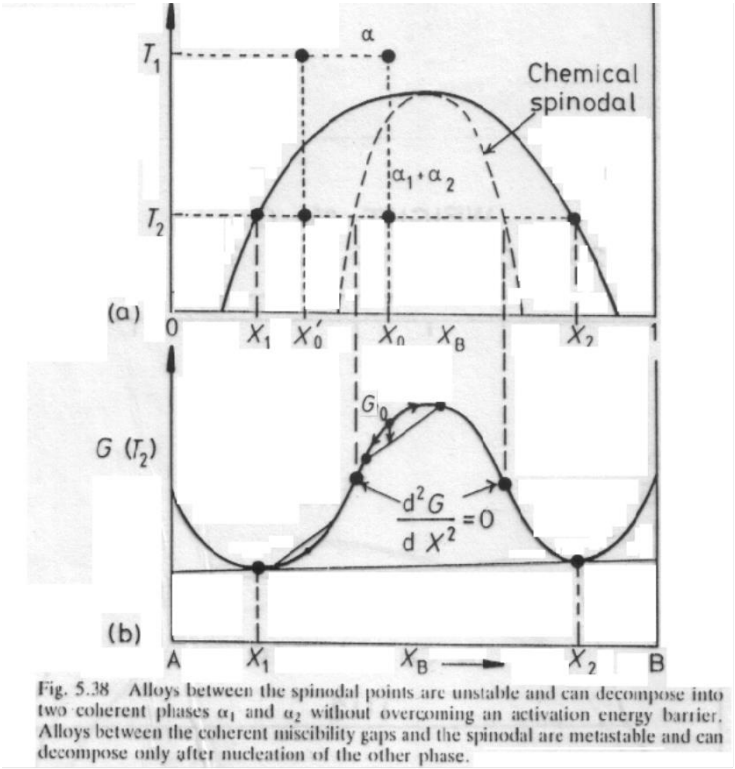

Fig. 5.38 Alloys between the spinodal points are unstable and can decompose into two coherent phases α_1 and α_2 without overcoming an activation energy barrier. Alloys between the coherent miscibility gaps and the spinodal are metastable and can decompose only after nucleation of the other phase.

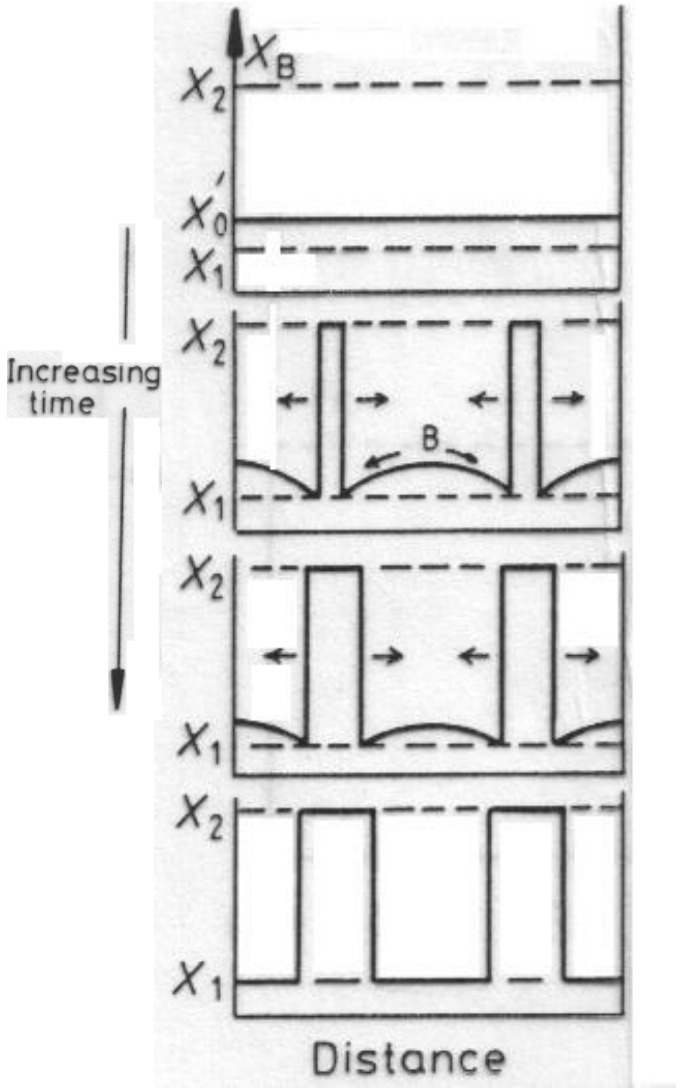

Spinodal decomposition

Composition fluctuation for alloy, X_0, within spinodal points: free energy gain with respect to G_0 stabilizes any compositional gradient (see arrow downwards). Transformation only due to diffusion.

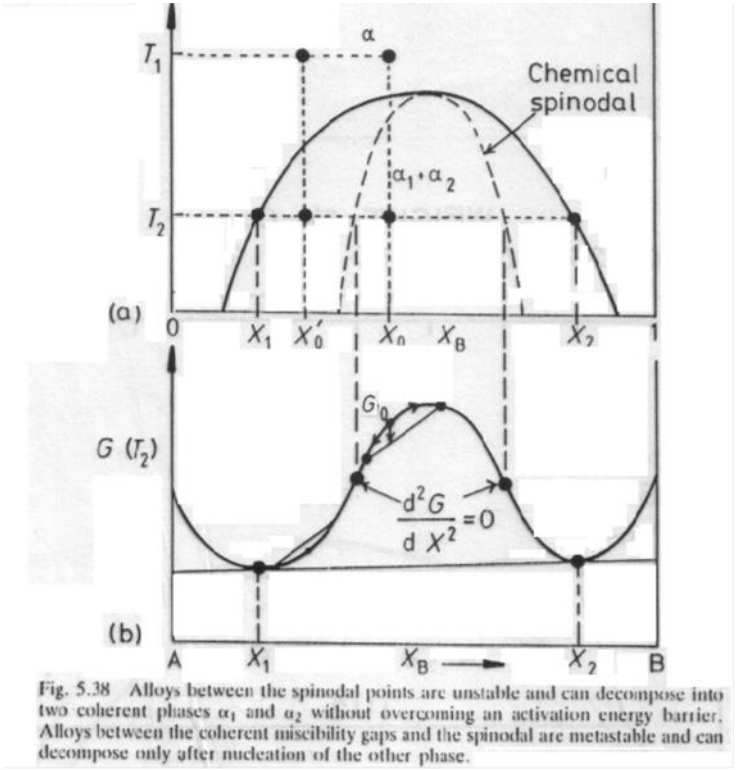

Fig. 5.38 Alloys between the spinodal points are unstable and can decompose into two coherent phases α_1 and α_2 without overcoming an activation energy barrier. Alloys between the coherent miscibility gaps and the spinodal are metastable and can decompose only after nucleation of the other phase.

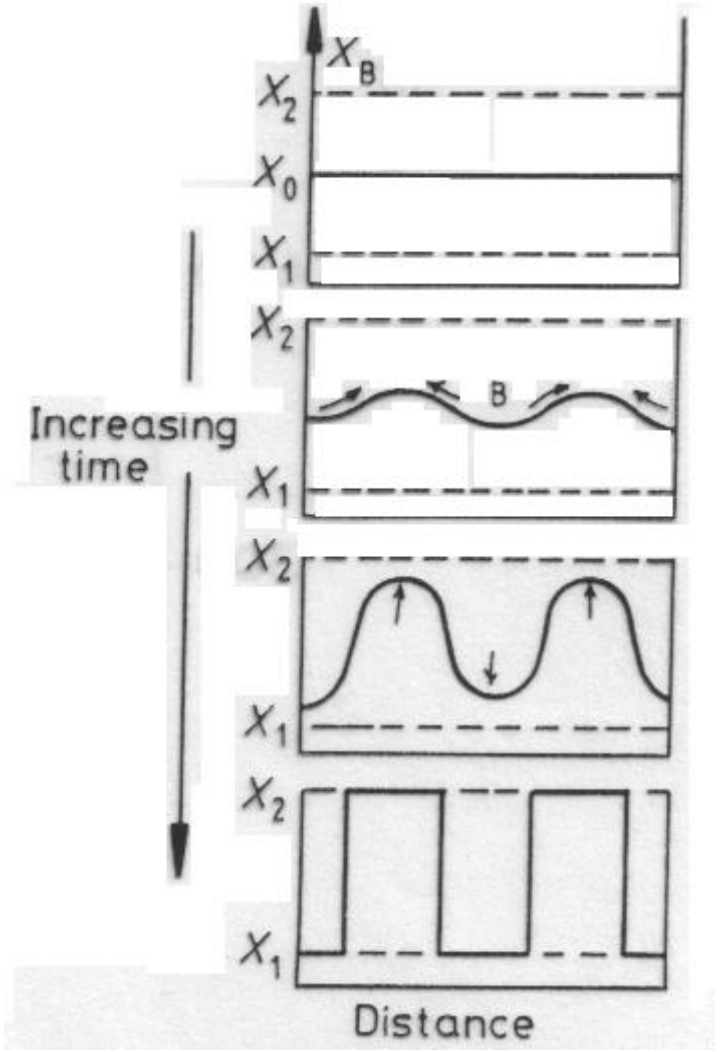

Massive transformation

In phase diagrams such as Cu-Zn, β → α transformation occurs via precipitation at low undercooling (as for γ → α in Fe-C, but with long range substitutional diffusion of Zn). **At high undercooling β → α is partitionless: α nucleates at gb's and grows into β via activated jumps across the interface**.

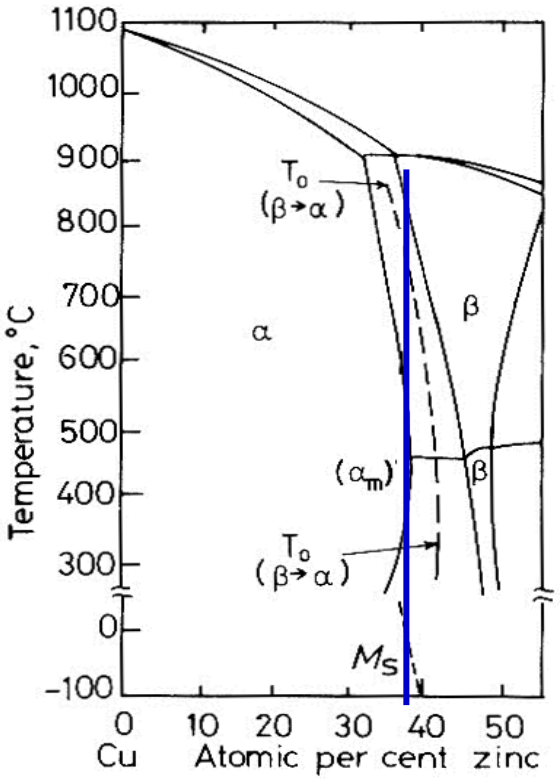

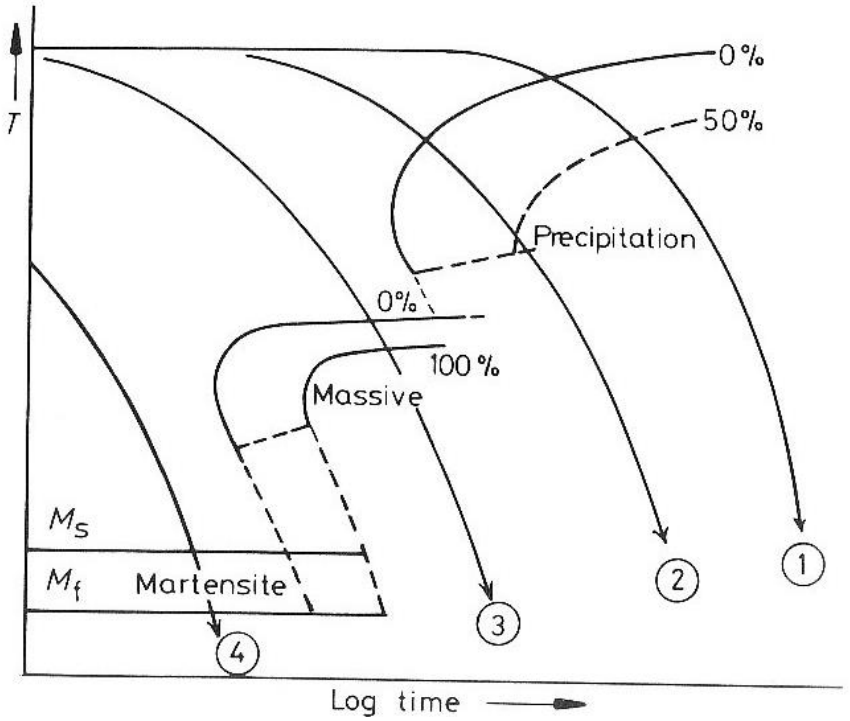

CCT and cooling curves. Martensitic transformation also possible at low temperature.

Massive transformation

Massive transformation occurs via gb's migration as for recrystallization but with high ΔG.

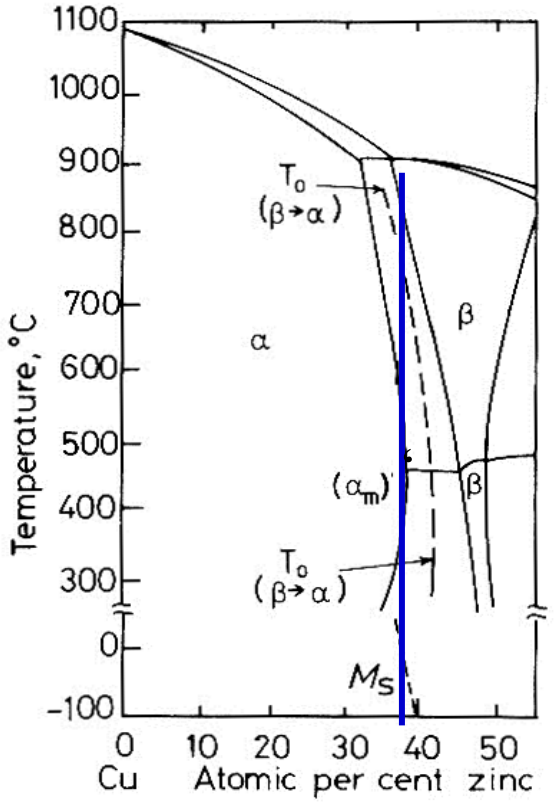

Massive transformation only possible below T_0 temperature, as explained in free energy scheme, where α and β have the same free energy.

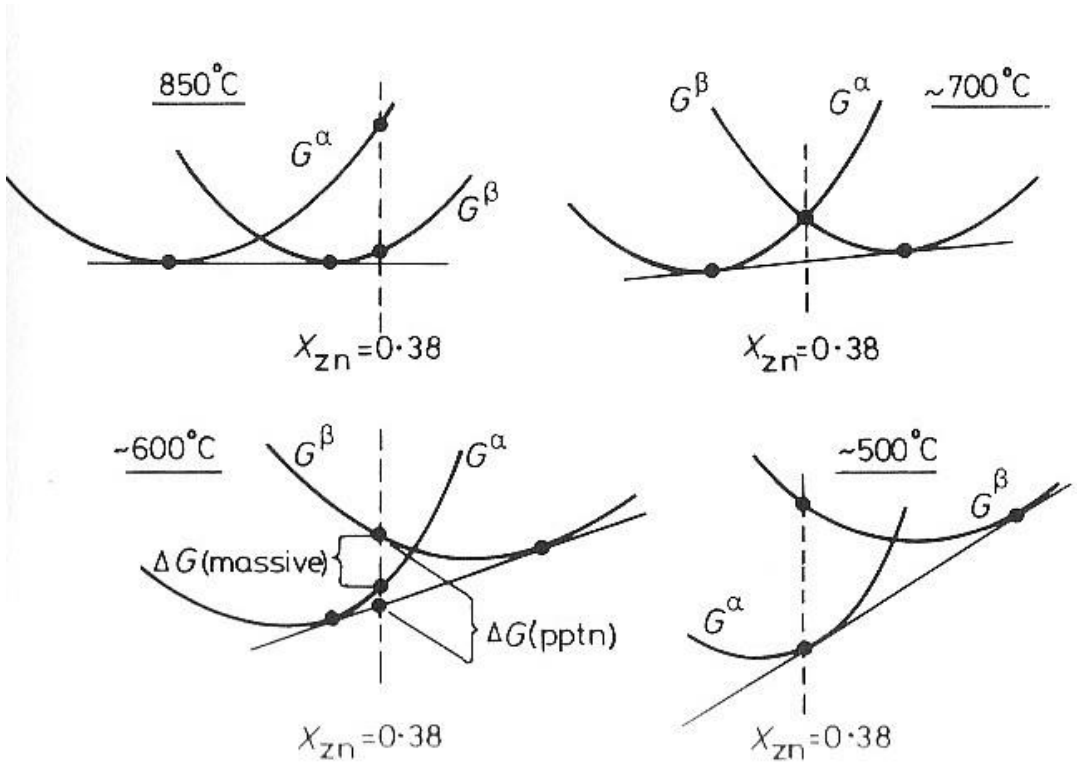

Ordering transformations

Ordered solutions (e. g. β' in Cu-Zn, CuAu and Cu3Au in Cu-Au) are described by means of sublattices where each atom sits (ex. Cu in A, Zn in B). Off-stoichiometry is accounted for by vacancies or excess solute (ex. Cu in Zn sites). **Order is expressed via a long-range *(L)* or short range *(s)* parameter**.

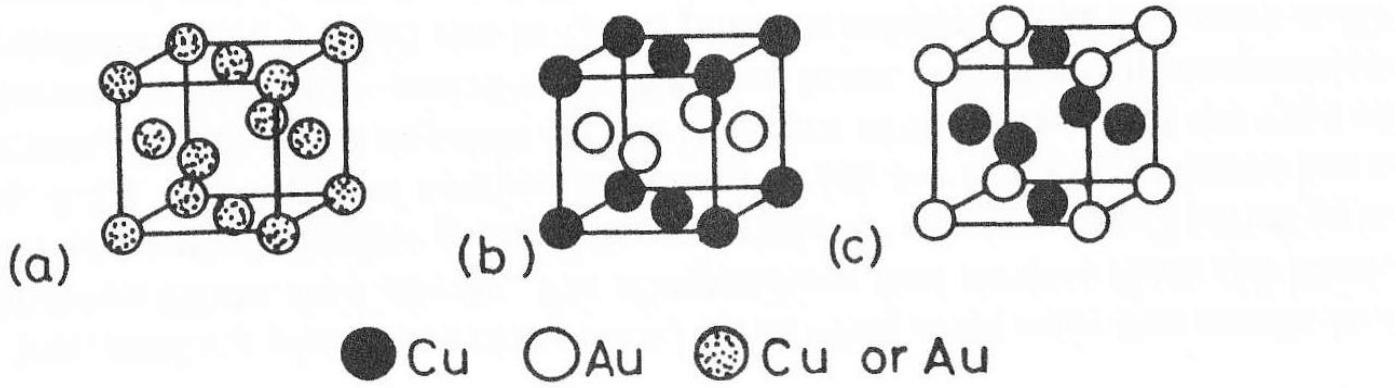

Fig. 1.20 Ordered substitutional structures in the Cu–Au system: (a) high-temperature disordered structure, (b) CuAu superlattice, (c) Cu_3Au superlattice.

Ordering transformations

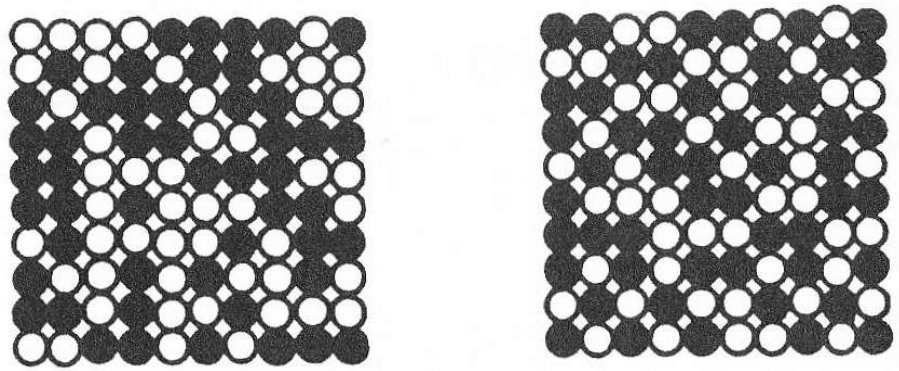

Fig. 1.19 (a) Random A–B solution with a total of 100 atoms and $X_A = X_B = 0.5$, $P_{AB} \sim 100$, $s = 0$. (b) Same alloy with short-range order $P_{AB} = 132$, $P_{AB(max)} \sim 200$, $s = (132 - 100)/(200 - 100) = 0.32$.

Short range order parameter

$$s = \frac{P_{AB} - P_{AB}(random)}{P_{AB}(max) - P_{AB}(random)}$$

P_{AB} → n. of AB bonds in the actual solution
P_{AB}(random) → n. of AB bonds in a random solution
P_{AB}(max)→ n. of AB bonds max in solution

Exists also in some liquids

Ordering transformations

long range order parameter $$L = \frac{r_A - X_A}{1 - X_A}$$

r_A: probability that A is on the right sublattice

L = 0 at critical temperature, T_C, s accounts for short range interactions also at higher temperature.

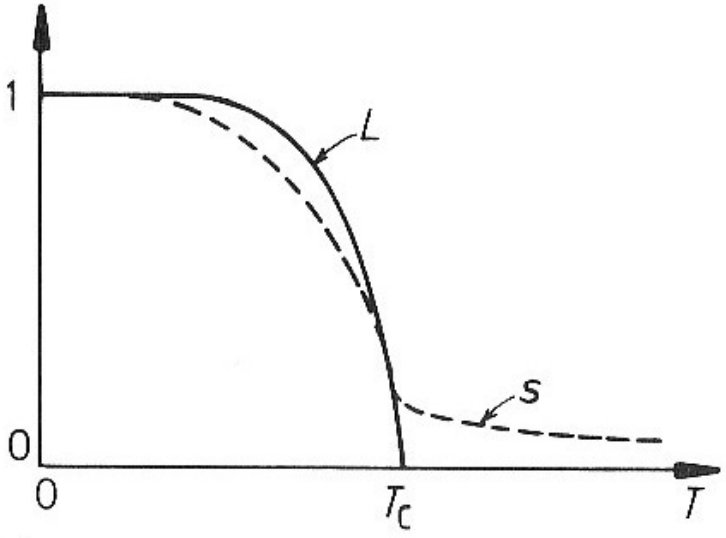

Ordering transformations

Order form either continuously (as in spinodal, when no latent heat exists) **or via nucleation and growth**.

Nucleation can be homogeneous because no change in composition occurs.

Each nucleus gives rise to a domain which grows independently. Impingement of domains may induce formation of anti-phase boundaries (APB).